Intertwined order in a frustrated four-leg $t − J$ cylinder

John F. Dodaro,[1,*] Hong-Chen Jiang,[2] and Steven A. Kivelson[1]

[1]*Department of Physics, Stanford University, Stanford, California 94305-4060, USA*

[2]*Stanford Institute for Materials and Energy Sciences, SLAC National Accelerator Laboratory and Stanford University, Menlo Park, California 94025, USA*

We report a density-matrix renormalization group study of the t-J model with nearest (t_1 and J_1) and next-nearest (t_2 and J_2) interactions on a four-leg cylinder with concentration $\delta = 1/8$ of doped holes. We observe an astonishingly complex interplay between uniform d-wave superconductivity (SC) and strong spin and charge-density wave ordering tendencies (SDW and CDW). Depending on parameters, the CDWs can be commensurate with period 4 or 8. By comparing the charge ordering vectors with $2k_F$, we rule out Fermi surface nesting-induced density wave order in our model. Magnetic frustration (i.e., $J_2/J_1 \sim 1/2$) significantly quenches SDW correlations with little effect on the CDW. Typically, the SC order is strongly modulated at the CDW ordering vector and exhibits d-wave symmetry around the cylinder. There is no evidence of a near-degenerate tendency to pair-density wave (PDW) ordering, charge $4e$ SC, or orbital current order.

I. INTRODUCTION

Theoretical context. It has become increasingly clear that the phase diagrams of highly correlated electronic systems are inherently complex, with multiple "intertwined" ordering tendencies [1] of comparable strength which sometimes appear to "compete" and sometimes peacefully coexist. The defining feature of such systems is that they involve a maximal degree of quantum frustration; neither the effective kinetic nor the interaction energy is dominant. Unfortunately, there are no controlled theoretical methods for solving generic "intermediate coupling" problems involving fermions in more than one spatial dimension (1D).

A partial solution is, however, possible: density matrix renormalization group (DMRG) methods [2–4] permit one to efficiently compute the ground-state properties of simple models, such as the t-J and Hubbard models, on ladder systems with the local geometry of any 2D lattice. Long enough ladders can be treated that confident extrapolation to the thermodynamic limit in one direction is possible, although the method is limited to ladders of at most modest width. To the extent that the properties we are interested in studying are generic properties of strongly correlated systems, we may hope that the solution of simple models, even where they do not faithfully represent the actual solid state chemistry of any particular material, can teach us something useful.

With this in mind, we have used the DMRG to explore the behavior of the lightly doped t-J model on the four-leg cylinder with first and second neighbor interactions. To explore the effects of band structure on the results, we study a range of values of the ratio of the nearest- and next-nearest-neighbor hopping matrix elements, t_1/t_2, while the effect of magnetic frustration is explored by varying the ratio of exchange constants, J_1/J_2. Since we are primarily focusing on density wave order, we report results at a fixed density of doped holes,

$\delta = 1/8$ (i.e., $1 − \delta = 7/8$ electrons per site), where these effects are particularly pronounced.

An empirical context. Various forms of charge-density wave (CDW) and spin-density wave (SDW) ordering tendencies have been documented in underdoped cuprate high temperature superconductors (as well as in many other interesting highly correlated materials) [5]. In some cases [6–8], as in LSCO, the CDW and SDW orders appear locked to each other in that they occur in the same ranges of "doped hole" concentration, δ (albeit with different onset temperatures), and with mutually commensurate ordering vectors. In other cases [9–11], as in YBCO, the CDW and SDW ordering tendencies seem to compete in that they appear (most strongly) in nonoverlapping ranges of δ and have ordering vectors that are unrelated to one another. This dichotomy has lead some to conclude [12] that there are two unrelated ordering tendencies in LSCO and YBCO, despite strong similarities in many other macroscopic signatures of these orders [13].

Basic issues of interpretation have also arisen concerning the driving force that gives rise to these density-wave orders. From a strong coupling perspective, CDW formation can arise as a consequence of a mesoscale tendency to phase separation [14–24]. Density wave order might also arise from specific features of the Fermi surface, including well nested portions of the Fermi surface [25] (although the validity of this perspective with *any* plausible band structure in more than one dimension has been strongly challenged [26]) or with putative "hot spots" on the Fermi surface [27–30] spanned by the ordering vector associated with (probably nonexistent) near quantum critical antiferromagnetic fluctuations.

II. RESULTS

Our principle results are summarized in the schematic phase diagrams in Figs. 1 and 2 and Table I, which pertain, respectively, to the cases with periodic and antiperiodic boundary conditions around the cylinder. (Antiperiodic boundary conditions are equivalent to a half-quantum of flux threaded through the cylinder, so these results are referred to as "flux.")
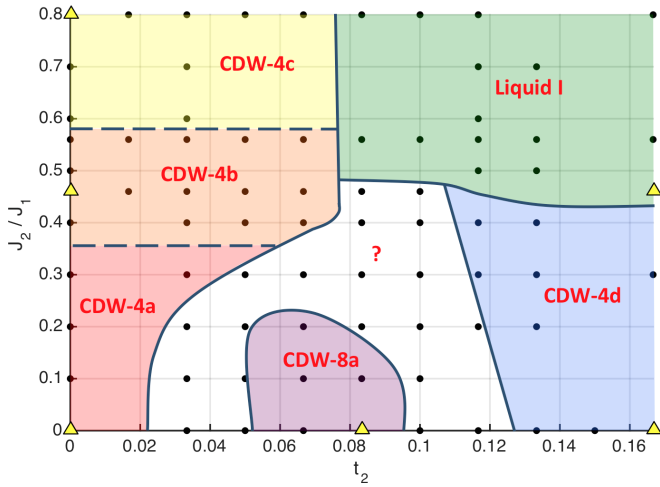
_____

*jdodaro@stanford.edu

FIG. 1. Phase diagram of the frustrated four-leg t-J cylinder with periodic boundary conditions for parameters $t_1 = 1$ and $J_1 = 1/3$. Solid lines represent schematic phase boundaries based on our data, and dashed lines indicate crossovers. The nature of the various phases and regimes is represented in Table I, where values for measured quantities are given for representative points in each region—indicated by the yellow triangles. Values of parameters for which calculations have been carried out are indicated by the dots. The phase diagram for $-1/6 \leqslant t_2 < 0$ is the same as for $t_2 = 0$.

(1) CDW phases. We find two distinct patterns of commensurate CDW long-range order: those with period 4 (CDW-4) and with period 8 (CDW-8). The corresponding ordering vectors are $\vec{Q}_{cdw} = 2\pi(1/4,0)$ for CDW-4 and $\vec{Q}_{cdw} = 2\pi(1/8,0)$ for CDW-8. Elsewhere in the phase diagram, the CDW correlations fall exponentially, except in the lower parts of the region marked "?," where there are weak but possibly power-law incommensurate correlations. We define the liquid phase as lacking CDW order.

(2) SDW correlations. Everywhere, except possibly in liquid I, the SDW correlations fall exponentially with distance. However, where the magnetic correlation length, ξ_{sdw}, is long
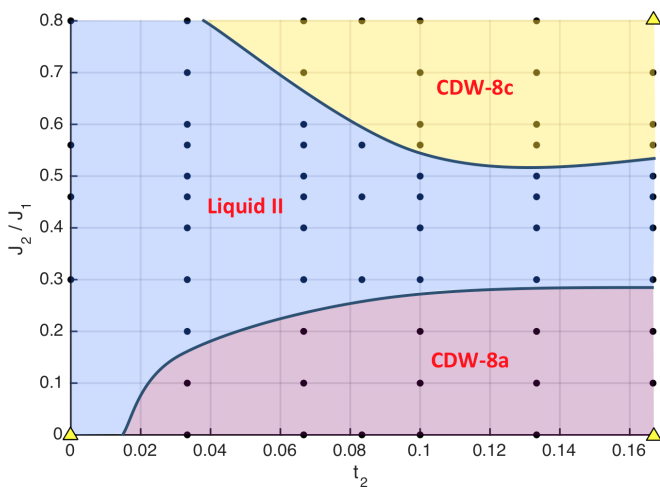

FIG. 2. Phase diagram of the frustrated four-leg t-J cylinder with antiperiodic boundary conditions (half quantum of flux) for parameters $t_1 = 1$ and $J_1 = 1/3$. Symbols are as in Fig. 1.

compared to $L_y/2 = 2$ lattice constants, this indicates a strong tendency toward antiferromagnetic order which might well correspond to true long-range order (LRO) in the 2D limit. (For comparison, note that the spin correlation length of the four-leg Heisenberg cylinder [31] is $\xi_{sdw} = 7a$, a length that increases exponentially [32] with the number of legs of the cylinder.)

We have divided the various phases into regimes according to the nature of the SDW correlations.

(2a) In CDW-4a, there is a tendency to SDW order with $\vec{Q}_{sdw} = 2\pi[3/8,1/2]$; this is the familiar "$t$-$J$ stripe" state discovered by White and Scalapino [20] in the four-leg ladder with $J_2 = t_2 = 0$ and eight-leg cylinder [24], which is highly reminiscent of the stripe order discovered earlier in the 214 family of cuprate high temperature superconductors [6]. The order here can be visualized as consisting of locally Néel order with antiphase domain walls coinciding with the location of lines of enhanced doped hole density.

(2b) With increasing magnetic frustration ($J_2 \sim J_1/2$), this phase gives way to CDW-4b, in which the CDW correlations are roughly unchanged, but the magnetic correlations fall exponentially with a length scale equal to a lattice constant or less. As far as we know, this behavior has not been previously observed in such calculations; it is more reminiscent of the CDW order seen [33–35] recently in the YBCO and BSCCO families of cuprate high temperature superconductors, where there is no low energy magnetism accompanying the CDW order.

(2c) For still stronger magnetic frustration ($J_2 \sim J_1$) a new form of short-range "spin-stripe" order appears in CDW-4c, with $\vec{Q}_{sdw} = 2\pi[0,1/2]$.

(2d) Increasing to $t_2 \sim t_1/6$ with small J_2 yields CDW-4d, a weak period 4 CDW with short-range $\vec{Q}_{sdw} = \pi[1,1]$ Néel antiferromagnetic correlations.

(2e) Similar distinctions exist in CDW-8. CDW-8a hosts magnetic correlations similar to those found in early Hartree-Fock studies of the Hubbard model [14,15]; here $\vec{Q}_{sdw} = 2\pi[7/16,1/2]$ corresponding to antiphase domain walls in a locally Néel order. As far as we know, this behavior has not been previously obtained in any non-mean-field calculations.

(2f) CDW-8c is a period 8 version of CDW-4c, in which short-range "spin-stripe" magnetism appears with $\vec{Q}_{sdw} = 2\pi[0,1/2]$.

(2g) The liquid phases lack CDW order but are distinguished by different spin correlations. Liquid I has quasi-long-range $(\pi,0)$ SDW order, while liquid II has exponentially decaying spin correlations.

(3) Superconducting correlations. While the Mermin-Wagner theorem precludes superconducting LRO, one might have hoped for power-law superconducting correlations; this is not seen in any range of parameters we have studied. However, in most of the phase diagram, short-range superconducting correlations are strong, and the corresponding correlation lengths are longer than ξ_{sdw}. As has been observed in previous studies of the t-J model [21,24,36], the superconducting correlations always have a d-wave character in a sense we make precise in Sec. VI B and Fig. 9.

The pair-field correlations additionally exhibit pronounced amplitude oscillations along the cylinder as can be seen, for

TABLE I. Characterization of the various phases and regimes shown in Figs. 1 and 2 for $t_1 = 1$, $J_1 = 1/3$, and $L_x = 48$. For each regime, values of the parameters characterizing all significant order parameters are given for representative values of t_2 and J_2; the notation "fl" indicates the case with antiperiodic boundary conditions (flux). $\vec{Q}_{cdw}$ and $\vec{Q}_{sdw}$ (measured in units of 2π with the lattice constant set to unity) correspond to the location of peaks in the density and magnetic structure factors, respectively; wave vectors indicated by (k_x, k_y) correspond to (quasi-)long-range order, while those written as $[k_x, k_y]$ correspond to short-range order but with a long enough correlation length that a clearly defined peak in the structure factor can be identified. ρ_{cdw} is the amplitude of the CDW long-range order extrapolated to the thermodynamic limit ($L_x \to \infty$; see Supplemental Material [44]). ξ_{sdw} is the spin correlation length and ξ_{sc} is the superconducting correlation length. $\Phi_{y,y}^{(dw)}/\Phi_{y,y}^{(sc)}$ is the ratio of the oscillating and uniform components of the pair-field correlation function as in Eq. (9). Δ_1 is the energy to add one particle to the ladder [see Eq. (15)].

	CDW-4a	CDW-4b	CDW-4c	CDW-4d	CDW-8a		CDW-8c	Liq. I	Liq. II
t_2/t_1 ; J_2/J_1	0 ; 0	0 ; 0.46	0 ; 0.80	1/6 ; 0	1/12 ; 0	1/6 ; 0 (fl)	1/6 ; 0.80 (fl)	1/6 ; 0.46	0 ; 0 (fl)
$\vec{Q}_{cdw}$	(1/4,0)	(1/4,0)	(1/4,0)	[1/4,0]	(1/8,0)	(1/8,0)	(1/8,0)		[1/8,0]
ρ_{cdw} (10^{-3})	~20	17(1)	10(2)	7(1)	~40	~40	14(3)	0.0(6)	0.0(3)
$\vec{Q}_{sdw}$	[3/8,1/2]		[0,1/2]	[1/2,1/2]	[7/16,1/2]	[7/16,1/2]	[0,1/2]	(1/2,0)	[5/12,1/2]
ξ_{sdw}	3.3(2)	0.80(4)	2.7(1)	3.0(2)	3.7(1)	2.4(7)	~4	~9	2.3(5)
ξ_{sc}	5.5	5.7	6.0	6.7	5.5	4.3	6.2	8.5	6.6
$\Phi_{y,y}^{(dw)}/\Phi_{y,y}^{(sc)}$	0.36	0.40	0.48	0.34	0.40	0.49	0.97	0.22	0.31
Δ_1	0.15	0.28	0.09	0.02	0.11	0.19			0.06

example, in Fig. 10(b). These oscillations have the same period as the CDW order, and reflect a strong coupling between CDW and SC order. We find no evidence of distinct finite momentum pair-density wave (PDW) ordering tendencies, which would be manifest [1] as oscillations with twice the period of the CDW [37].

(4) Other correlations. Following a suggestion of Affleck [40], we looked for evidence of charge 4e superconducting correlations. Also, to look for indications of $\vec{Q} = \vec{0}$ orbital loop order [41] and $\vec{Q} = \pi(1,1)$ d-density wave order [42], we computed the current-current correlation function. In all cases, these correlation functions fall to below our error limit within a couple of lattice constants. We thus cannot be more quantitative than to conclude that all of these ordering tendencies appear to be extremely weak in the present model.

(5) Relation to "fermiology." To explore the relation between the CDW ordering vector and the structure of the underlying Fermi surface, we need a prescription for determining the locations of the Fermi points, $\vec{k}_F$, for any bands that cross the Fermi surface. "Bare" values of $\vec{k}_F$ can be computed as a function of t_2/t_1 by ignoring all interactions, including the t-J constraint of no double occupancy. The physical (renormalized) locations of Fermi points are identified as values of the crystal momenta at which the fermion occupation probability, $\langle n_{\vec{k}\sigma} \rangle$, has a precipitous drop [43]. In Fig. 7, we compare the values of $2\vec{k}_F$ computed either way with the observed values of $\vec{Q}_{cdw}$ and $\vec{Q}_{sdw}$; we see that there is no obvious relation between the fermiology and the density wave ordering vectors.

Road map. In Sec. III, we present the model and define the correlation functions of interest. In Sec. IV, we present the results from DMRG for the charge and spin correlations in various regions of the ground state phase diagram. Section V describes calculations of single-particle correlation functions, from which we extract renormalized values of Fermi vectors, $\vec{k}_F$. Superconducting correlations and energy gaps are discussed in Secs. VI and VII respectively. A further discussion of the results is given in Sec. VIII.

III. MODEL

We treat the t-J model Hamiltonian with up to next-nearest neighbor interactions:

$$H = \mathcal{T}_1 + \mathcal{T}_2 + \mathcal{H}_1 + \mathcal{H}_2. \quad (1)$$

The kinetic energy term $\mathcal{T}_a$ is

$$\mathcal{T}_a = -t_a \sum_{\sigma, \langle ij \rangle_a} (e^{iA_{ij}} c_{i\sigma}^\dagger c_{j\sigma} + \text{H.c.}), \quad (2)$$

where $c_{i\sigma}^\dagger$ creates a fermion with spin polarization σ at site $\vec{r}_i = (x_i, y_i)$, A_{ij} is the integral of the gauge field from site i to j (in appropriate units), and $a = 1$ and 2 for nearest- and next-nearest-neighbor sites, respectively. The exchange term $\mathcal{H}_a$ is

$$\mathcal{H}_a = J_a \sum_{\langle ij \rangle_a} \left(\mathbf{S}_i \cdot \mathbf{S}_j - \frac{1}{4} n_i n_j \right), \quad (3)$$

where $n_i = \sum_\sigma n_{i,\sigma} = \sum_\sigma c_{i\sigma}^\dagger c_{i\sigma}$ is the occupation at site $\vec{r}_i$ and $\mathbf{S}_i = (1/2) c_{i\alpha}^\dagger \boldsymbol{\sigma}_{\alpha\beta} c_{i\beta}$ for Pauli matrices $\boldsymbol{\sigma}$.

There are $N = L_x \times L_y$ sites on the lattice, and the number of electrons would be $N_e = N$ at half filling, i.e., at $\delta \equiv [N - N_e]/N = 0$. We will take an electron concentration such that $\delta = 1/8$. The lattice geometry is of four-leg cylinders ($L_y = 4$) of lengths up to $L_x = 48$ with periodic and open boundary conditions along $\hat{y}$ and $\hat{x}$, respectively. In our calculations we set $t_1 = 1$ as energy unit and $J_1 = 1/3$, and keep up to $m = 6561$ number of states in each DMRG block with truncation errors $\epsilon_{\text{tr}} \leqslant 5 \times 10^{-6}$.

When there is no flux through the cylinder, we work in a gauge such that $A_{ij} = 0$. For the "fl" case, the sum of A_{ij} along any loop that encircles the cylinder once is equal to π; so as to work with a real Hamiltonian, in this case we chose a gauge such that $A_{ij} = 0$ on all bonds other than those connecting the two sides of one rung of the cylinder, for which $A_{ij} = \pi$.

$\langle n_{\vec{k}\sigma} \rangle$. In terms of the Fourier transform of the electron creation operator $c_{j\sigma}^{\dagger}$

$$c_{\vec{k}\sigma}^{\dagger} = \frac{1}{\sqrt{N}} \sum_j e^{i\vec{k}\cdot\vec{r}_j} c_{j\sigma}^{\dagger}, \qquad (4)$$

we can calculate the momentum occupation:

$$\langle n_{\vec{k}\sigma} \rangle = \langle c_{\vec{k}\sigma}^{\dagger} c_{\vec{k}\sigma} \rangle = \frac{1}{N} \sum_{i,j} e^{i\vec{k}\cdot(\vec{r}_i-\vec{r}_j)} \langle c_{i\sigma}^{\dagger} c_{j\sigma} \rangle. \qquad (5)$$

$S_{cdw}(\vec{k})$. The CDW structure factor is the Fourier transform of the density-density correlation function

$$S_{cdw}(\vec{k}) = \frac{1}{N} \sum_{i,j} e^{i\vec{k}\cdot(\vec{r}_i-\vec{r}_j)} \langle (n_i - \overline{n})(n_j - \overline{n}) \rangle, \qquad (6)$$

where $\overline{n} = 1 - \delta$ is the average particle density. Because the ends of the cylinders break translation symmetry, where there is long-range commensurate charge order, its amplitude, ρ_{cdw}, can be inferred from the amplitude of the oscillations of $\langle n_i \rangle$ near the middle of the cylinder [44], extrapolated to the $L_x \rightarrow \infty$ limit; the wave vector of these oscillations, $\vec{Q}_{cdw}$, always corresponds to a pronounced peak in the structure factor $S_{cdw}(\vec{k})$.

$S_{sdw}(\vec{k})$. The SDW structure factor is

$$S_{sdw}(\vec{k}) = \frac{1}{N} \sum_{i,j} e^{i\vec{k}\cdot(\vec{r}_i-\vec{r}_j)} \langle \mathbf{S}_i \cdot \mathbf{S}_j \rangle.$$

We obtain the correlation length, ξ_{sdw}, by fitting the long-distance fall-off of spin-spin correlation function, $\langle \mathbf{S}_i \cdot \mathbf{S}_j \rangle$, to an exponential. This approach fails only if the correlation length is comparable or longer than the system size, or if the correlations fall with a power law [45]. We use the somewhat arbitrary criterion, $\xi_{sdw} > L_y/2 = 2$, as the definition of "significant" SDW correlations.

Φ_{sc}. The singlet superconducting pair-field creation operator on neighboring pairs of sites is defined as

$$\phi_{\vec{a}}^{\dagger}(\vec{r}_i) = \frac{1}{\sqrt{2}} (c_{i\uparrow}^{\dagger} c_{i+a\downarrow}^{\dagger} - c_{i\downarrow}^{\dagger} c_{i+a\uparrow}^{\dagger}), \qquad (7)$$

where $\vec{a} = \hat{x}, \hat{y}$, and $\hat{x} + \hat{y}$ corresponds to different singlet orientations. The primary diagnostic of SC order we have analyzed is the pair-field correlator,

$$\Phi_{a,a'}(\vec{r},\vec{r}\,') = \langle \phi_{\vec{a}}^{\dagger}(\vec{r}) \phi_{\vec{a}'}(\vec{r}\,') \rangle, \qquad (8)$$

which in all cases we have studied, for large separations along the ladder, $1 \ll |x| \ll L_x$, where $\vec{r} - \vec{r}\,' = x\hat{x} \equiv \vec{X}$, Φ can be expressed as the sum of a uniform and an oscillatory piece as

$$\Phi_{a,a'}(\vec{r},\vec{r}\,') \sim \left\{ \Phi_{a,a'}^{(sc)} + \Phi_{a,a'}^{(dw)} \cos[\vec{Q}_{cdw} \cdot \vec{X} + \theta_0] \right\} e^{-|\vec{X}|/\xi_{sc}}, \qquad (9)$$

from which we derive the values for $\Phi_{y,y}^{(sc)}/\Phi_{y,y}^{(dw)}$ and ξ_{sc} quoted in Table I and elsewhere. If there are superconducting correlations that oscillate with any other wave vectors, i.e., any PDW ordering tendencies, they are either too weak or too short-ranged to be observable in our calculations. We have looked for SC correlations in a complimentary fashion by applying an external field $D_{\vec{a}}(\vec{r}_i) \sim (\phi_{\vec{a}}^{\dagger}(\vec{r}_i) + \phi_{\vec{a}}(\vec{r}_i))$ to

the boundary of the ladder, and then measured the induced pair-field expectation values $\langle D_{\vec{a}}(\vec{r}_i) \rangle$, as a function of distance from this rung. Results obtained in this manner are broadly consistent with those obtained from the analysis of Φ.

Other orders. To search for charge 4e superconducting correlations, we have computed the correlation functions of the two singlet "quartet" creation operators,

$$\phi_{4e,+}^{\dagger} = \frac{1}{2}(c_{1\uparrow}^{\dagger} c_{2\downarrow}^{\dagger} c_{3\downarrow}^{\dagger} c_{4\uparrow}^{\dagger} - c_{1\uparrow}^{\dagger} c_{2\uparrow}^{\dagger} c_{3\uparrow}^{\dagger} c_{4\downarrow}^{\dagger}$$
$$- c_{1\uparrow}^{\dagger} c_{2\uparrow}^{\dagger} c_{3\downarrow}^{\dagger} c_{4\downarrow}^{\dagger} - c_{1\downarrow}^{\dagger} c_{2\downarrow}^{\dagger} c_{3\uparrow}^{\dagger} c_{4\uparrow}^{\dagger}), \qquad (10)$$

$$\phi_{4e,-}^{\dagger} = \frac{1}{\sqrt{12}}(2c_{1\uparrow}^{\dagger} c_{2\downarrow}^{\dagger} c_{3\downarrow}^{\dagger} c_{4\uparrow}^{\dagger} + 2c_{1\downarrow}^{\dagger} c_{2\uparrow}^{\dagger} c_{3\uparrow}^{\dagger} c_{4\downarrow}^{\dagger}$$
$$- c_{1\uparrow}^{\dagger} c_{2\downarrow}^{\dagger} c_{3\uparrow}^{\dagger} c_{4\downarrow}^{\dagger} - c_{1\downarrow}^{\dagger} c_{2\uparrow}^{\dagger} c_{3\downarrow}^{\dagger} c_{4\uparrow}^{\dagger}$$
$$- c_{1\uparrow}^{\dagger} c_{2\uparrow}^{\dagger} c_{3\downarrow}^{\dagger} c_{4\downarrow}^{\dagger} - c_{1\downarrow}^{\dagger} c_{2\downarrow}^{\dagger} c_{3\uparrow}^{\dagger} c_{4\uparrow}^{\dagger}), \qquad (11)$$

which are defined on each plaquette around which we label the sites 1-2-3-4 starting in the bottom left corner and moving counterclockwise.

To check for possible loop current or d-density wave order, we measured the current-current correlation function for current operator $J_{pq}^{\sigma} = -i(c_{p,\sigma}^{\dagger} c_{q,\sigma} - c_{q,\sigma}^{\dagger} c_{p,\sigma})$ with sites p and q along $\hat{x}$ and $\hat{y}$ bonds and found exponentially decaying correlations with $\xi_{\text{loop}} < 2$ across the phase diagram indicating loop current order is unlikely in our model within the range of parameters explored [46].

IV. PHASE DIAGRAM

In the limit $\delta = 0$, the present model reduces to an insulating spin-1/2 Heisenberg quantum antiferromagnet, so it is reasonable to view the present system as being a doped antiferromagnet. The ground state of the spin 1/2 Heisenberg antiferromagnet on the 2D square lattice with J_2/J_1 small is known to have Néel ($\vec{Q}_{sdw} = [\pi,\pi]$) order, while for large enough J_2/J_1 it has "stripe antiferromagnetic" ($\vec{Q}_{sdw} = [\pi,0]$ or $[0,\pi]$) order. For $J_2/J_1 \sim 1/2$, previous studies [47–50] have established the existence of a quantum paramagnetic phase with a spin gap and tentatively concluded [48] that there is a spin liquid for $J_2/J_1 = 0.41$–0.5 and a valence bond solid for $J_2/J_1 = 0.5 - 0.62$. Thus the doped ladder with $J_2/J_1 \sim 1/2$ can be viewed as a doped quantum paramagnet.

The ground-state phase diagrams for $\delta = 1/8$ extracted from our DMRG results are shown in Figs. 1 and 2, and reported in Table I. In this section we give a taste of the explicit analysis that leads to the conclusions summarized there.

Analysis for $J_2 \approx 0$. The density profile $\langle n(x) \rangle = (1/L_y) \sum_y \langle n(x,y) \rangle$ for $J_2 = 0$ and different values of t_2 are shown in Fig. 3(a) for the central 32 sites of the 48×4 system. The commensurate period 4 CDW-4a with ordering vector $\vec{Q}_{cdw} = 2\pi(2\delta,0)$ is stable at least for $-1/6 \leqslant t_2 \lesssim 0.02$. Expressed in terms of a picture of charge stripes, there are two holes per stripe or $\rho = 1/2$ holes per domain wall unit cell ("half-filled stripes"). The largest CDW amplitude occurs for the period 8 [$\vec{Q}_{cdw} = 2\pi(\delta,0)$, i.e., $\rho = 1$] in a range of $t_2 \sim 1/12$ identified as CDW-8a. For larger t_2, the period 4 CDW order is weakened; we refer to this phase as CDW-4d.
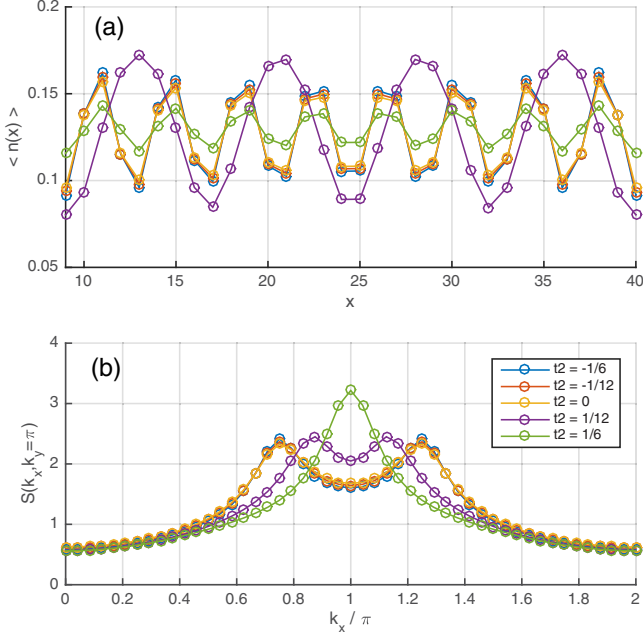
FIG. 3. (a) Density profile and (b) spin structure factor at $k_y = \pi$ for $J_2 = 0$ and $t_2 = 0, \pm 1/12, \pm 1/6$ for the t-J model without flux.
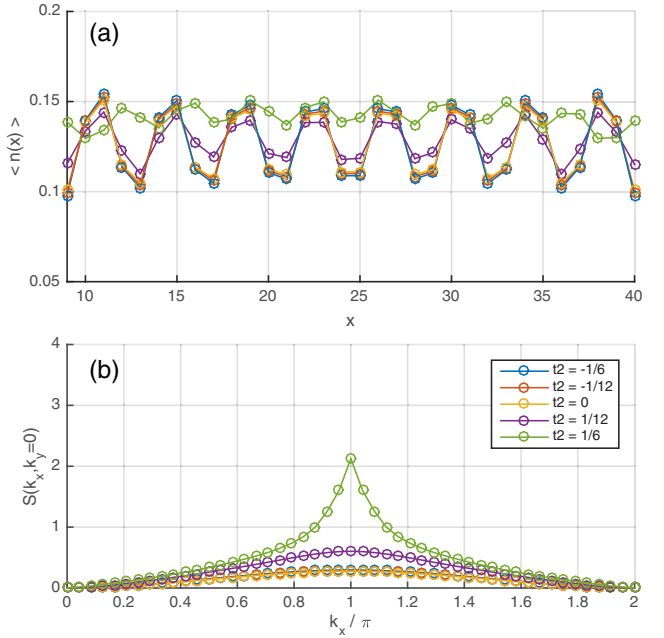

FIG. 4. (a) Density profile and (b) spin structure factor at $k_y = 0$ for $J_2 = 0.46 J_1$ and $t_2 = 0, \pm 1/12, \pm 1/6$ for the t-J model without flux. The apparent oscillation of the density profile for $t_2 = 1/6$ vanishes in the $L_x \to \infty$ limit (see Supplemental Material [44]).

The $J_2 = 0$ spin structure factor as a function of k_x is shown for different t_2 in Fig. 3(b) for $k_y = \pi$. In CDW-4a (for small $t_2 > 0$) the magnetic structure factor has a pronounced peak $\vec{Q}_{sdw} = \vec{Q}_{AF} \pm \Delta \vec{Q}$ where $Q_{AF} = \pi(1,1)$ and the antiferromagnetic incommensurability is $\Delta \vec{Q} = \pi(2\delta, 0)$. CDW-8a ($t_2 \sim 1/12$) has local magnetic correlations corresponding to a SDW with antiferromagnetic incommensurability $\Delta \vec{Q} = \pi(\delta, 0)$. The antiferromagnetic incommensurability disappears for $t_2 = 1/2$ (CDW-4d) where the system exhibits short-ranged Néel ordered with spin-spin correlation length $\xi_{sdw} \sim 3.0$.

Turning now to the cylinder threaded with a half-flux quantum (i.e., the results in Fig. 2) for $t_2 \approx 0$, charge order vanishes in the $L_x \to \infty$ limit. The magnetic structure factor exhibits a peak away from $\vec{Q}_{AF}$ with antiferromagnetic incommensurability $\Delta \vec{Q} = \pi(1/6, 0)$; as these correlations are exponentially decaying, we identify this phase as liquid II to draw a distinction with liquid I which may possess power-law correlations. Upon increasing t_2, the CDW-8a phase is stabilized with a large amplitude that increases with t_2.

Analysis for $J_2 \sim J_1/2$. Next, we treat $J_2 = 0.46 J_1$, corresponding to the quantum paramagnet phase in the undoped 2D system. We find a nearly identical period 4 CDW for $-1/6 \leqslant t_2 \lesssim 1/12$ in Fig. 4(a), but a vanishing of SDW order as seen in Fig. 4(b) with $\xi_{sdw} < 1$; this corresponds to CDW-4b in Fig. 1. The period 8 CDW is absent for $J_2 = 0.46 J_1$ at $t_2 \sim 1/12$, and for $1/12 < t_2 \leqslant 1/6$ we find quasi-long-ranged $(\pi, 0)$ antiferromagnetism and vanishing CDW order; we refer to this phase as liquid I. Similar features were seen for $J_2 = 0.56 J_1$, where in the undoped 2D case there may be a valence bond solid state.

Turning again to the flux case, we find the liquid II phase for $0 \leqslant t_2 \leqslant 1/6$ which lacks pronounced peaks in both density and magnetic structure factors.

Analysis for $J_2 \sim J_1$. In the 2D undoped system, $J_2 = 0.80 J_1$ lies in the phase exhibiting stripe antiferromagnetism. Here we find a weaker period 4 CDW for $-1/6 \leqslant t_2 \lesssim 1/12$ and a short-ranged $[0, \pi]$ SDW (labeled as CDW-4c in Table I). Increasing $t_2 > 1/12$ results in quasi-long-ranged $(\pi, 0)$ SDW which again shows no apparent CDW order (liquid I phase) as seen in Fig. 5.

Turning to the flux case, we find a period 8 CDW for $t_2 \gtrsim 1/30$ accompanied by a short-ranged $[0, \pi]$ SDW labeled as CDW-8c phase.

It is apparent that the phase diagrams with periodic and antiperiodic boundary conditions (Figs. 1 and 2, respectively) differ significantly suggesting finite L_y effects are still substantial on the four-leg cylinder; this observation precludes a reliable extrapolation of these results to the 2D thermodynamic limit. The 1D thermodynamic limit $L_x \to \infty$ can be studied, and details on this extrapolation can be found in the Supplemental Material [44].

V. BAND STRUCTURE

To understand the role of band structure on the results, we have studied the ground state properties for different values of the ratio of nearest- and next-nearest-neighbor hopping matrix elements t_2/t_1. The noninteracting band structure is

$$E(\vec{k}) = -2t_1[\cos(k_x) + \cos(k_y)] - 4t_2[\cos(k_x)\cos(k_y)] - \mu, \quad (12)$$

where μ is the chemical potential. For the four-leg cylinder in the $L_x \to \infty$ limit, the (1D) Bloch wave vector $k \equiv k_x$ takes on all values between $-\pi$ and π, while the discrete allowed values of k_y serve as band indices; in the flux-free cylinder
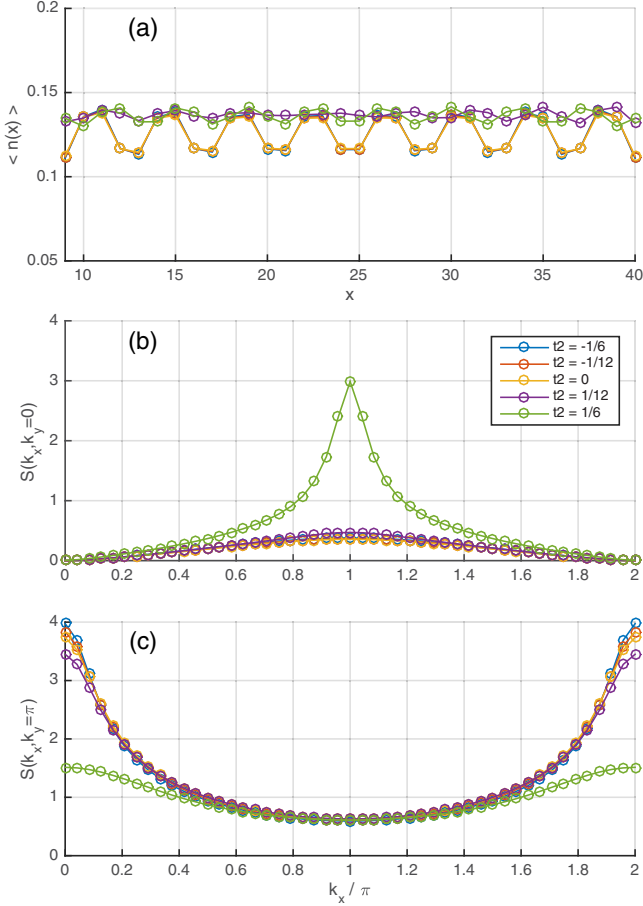
FIG. 5. (a) Density profile and spin structure factor at (b) $k_y = 0$ and (c) $k_y = \pi$ for $J_2 = 0.80J_1$ and $t_2 = 0, \pm 1/12, \pm 1/6$ for the t-J model without flux.
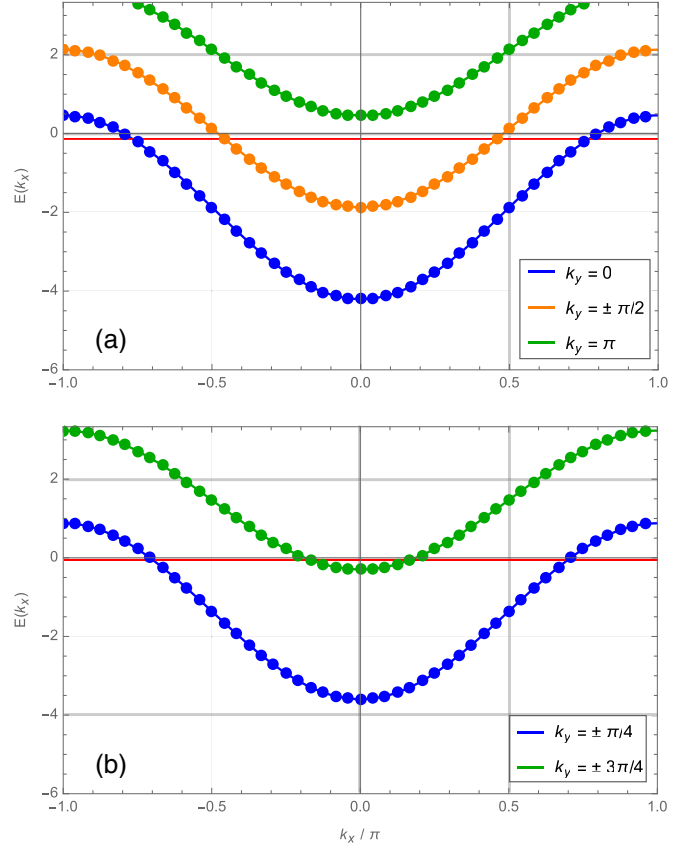

FIG. 6. Band structure of noninteracting model [see Eq. (12)] at $t_1 = 1$, $t_2 = 1/12$, $\delta = 1/8$ with (a) periodic and (b) antiperiodic boundary conditions.

(periodic BCs), the allowed values of k_y are $k_y = \{0, \pm \pi/2, \pi\}$, while for antiperiodic BCs (fl) $k_y = \{\pm \pi/4, \pm 3\pi/4\}$. The corresponding band structures for periodic and antiperiodic BCs at $t_2 = 1/12$ are shown in Figs. 6(a) and 6(b), respectively, where the horizontal red line indicates the Fermi energy for $\delta = 1/8$. The center band is doubly degenerate for periodic BC, and both bands are doubly degenerate for antiperiodic BC.

In the interacting problem, as well, Bloch's theorem allows us to identify bands labeled by a band index, corresponding to the above values of k_y, and a 1D Bloch wave-vector, k, corresponding to k_x. Although Fermi liquid theory does not apply in 1D, in some cases a Fermi surface can be identified from a calculation of the single-electron occupation probability, $\langle n_{\vec{k},\sigma} \rangle$, if it has a nonanalyticity at $\vec{k} = k_F(k_y)\hat{x} + k_y\hat{y}$. However, in practice it is difficult to distinguish a nonanalyticity from a rapid analytic change. Thus, as an operational definition of the Fermi momenta of the interacting system, we identify Fermi surface crossings with cases in which $\langle n_{\vec{k},\sigma} \rangle$ drops sharply and the corresponding value of k_F is associated with points of maximal slope, i.e., points at which $d^2\langle n_{\vec{k}\sigma} \rangle/dk^2 = 0$ [43].

A so-called "generalized Luttinger's theorem [51]," which is really a generalized form of the Leib-Schulz-Mattis theorem

[52], requires that in the absence of symmetry breaking, there must be a gapless neutral mode of the system with wave vector $Q_{\text{Lutt}} \equiv 4\pi(1 - \delta)$, which can be thought of as the almost Goldstone mode of an incommensurate CDW. In contrast with Luttinger's theorem for Fermi liquids in more than 1D, this construction makes no direct reference to the single-particle spectrum at all. However, if this could be interpreted in terms of fermiology, it would correspond to the "total" value

$$k_F^{\text{eff}} = \sum_{k_y} k_F(k_y) \rightarrow \frac{Q_{\text{Lutt}}}{2} = 2\pi(1 - \delta). \qquad (13)$$

To study the possible origin of density wave order through Fermi surface nesting, we compare the charge ordering vector Q_{cdw} to the noninteracting and interacting $2k_F(k_y)$ for each band. The values of Q_{cdw} are compared with the values of $2k_F$ in Fig. 7. The noninteracting $2k_F$'s are represented by open triangles and the interacting $2k_F$'s by filled diamonds. We see that the ordering wave vectors do not coincide with $2k_{F_i}$ for each band which rules out CDW induced by Fermi surface nesting in our system. Similar results are found across the $t_2 - J_2$ phase diagram suggesting another mechanism is responsible for the observed phases. Additionally the noninteracting k_F do not agree with the interacting k_F showing a weak coupling perspective is not applicable to our results.

We had hoped to identify cases in which this inference is violated in such a way that $k_F^{\text{eff}} = (4\pi/2)\delta$; this, in turn,
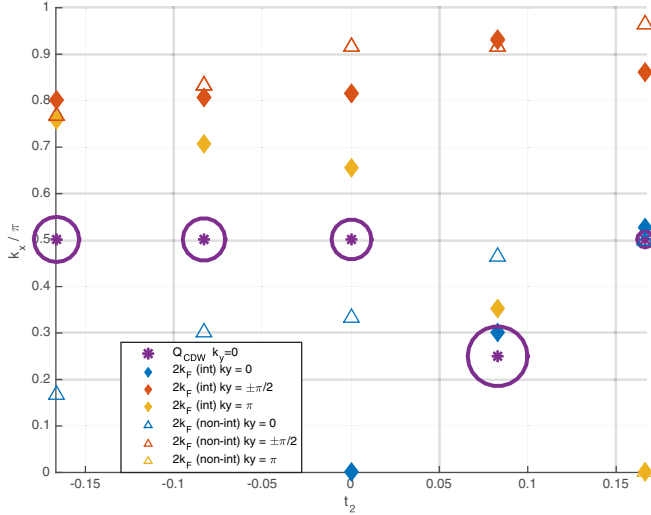
FIG. 7. Charge ordering vectors and $2k_{F_i}$ for the t-J model with $J_2 = 0$, $L_x = 48$, and periodic boundary conditions at $t_2 = 0, \pm 1/12, \pm 1/6$. Open triangles and filled diamonds represent noninteracting and interacting $2k_{F_i}$, respectively.

FIG. 8. Superconducting correlations may have (a) d-wave symmetry characterized by a change in sign (color) of the order parameter *around* the cylinder or (b) d-wave-like which has s-wave symmetry around the cylinder, but changes sign about plaquettes along the cylinder.

might have been suggestive of a tendency toward an exotic topologically order Fermi liquid phase (known as FL*), such as can occur [53–55] in certain versions of the quantum dimer model [56]. However, wherever well-defined Fermi surface crossings can be identified in our data, we find that they are suggestive of the Luttinger relation in Eq. (13).

VI. SUPERCONDUCTING CORRELATIONS

A. Charge 2e

We study charge $2e$ superconducting order by measuring the pair-field correlation function $\Phi_{a,a'}(\vec{r},\vec{r}\,')$ as defined in Eq. (8). We find that $\Phi_{x,x}$, $\Phi_{y,y}$, $\Phi_{x,y}$, and $\Phi_{x+y,x+y}$ all decay exponentially although we focus on $\Phi_{y,y}$ as it tends to have the largest amplitude. We do not find quasi-long-range superconducting order in our study; however, we can still make qualitative statements about the relation between competing orders. As noted earlier, increasing t_2 results in a weakening of charge order while maintaining Néel or stripe antiferromagnetic order depending on J_2. The $J_2 = 0$ superconducting correlations increase slightly from $\xi_{sc} \approx 5.5$ to $\xi_{sc} \approx 6.7$ as t_2 increases from zero to $1/6$. This enhancement of superconducting correlations with increasing t_2 (accompanied with weakening of CDW) suggests a competition between superconductivity and charge order. We find pronounced amplitude oscillations in the superconducting correlation functions with the same period as the CDW which will be discussed below.

Compared with the periodic boundary condition, there is a clear enhancement of charge $2e$ superconducting correlations for the case with antiperiodic boundary conditions (flux). We find the largest correlation lengths for $J_2/J_1 = 0.3$ and 0.46 corresponding to the quantum paramagnet with no spin and charge order (liquid II phase). For these values of J_2, the superconducting correlations appear more uniform with a correlation length of $\xi_{sc} \sim 10$ for $J_2/J_1 = 0.3$ and $t_2 = 1/6$ shown in Fig. 10(a). This enhancement of uniform super-
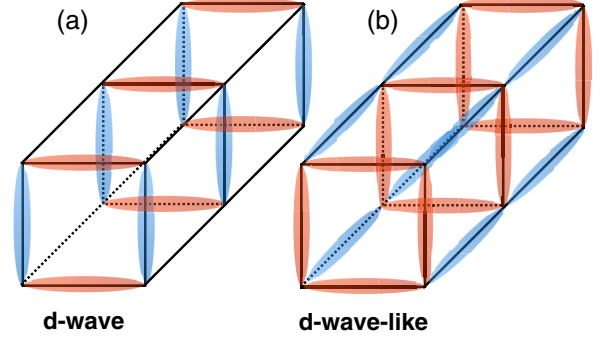
conducting correlations coinciding with the destabilization of stripes (by flux and magnetic frustration) serves as additional evidence for a competition between these orders.

B. Pair symmetry

Although the locally d-wave character of the superconducting correlations has long been noted in DMRG studies of t-J ladders [21,36], in the cylinder geometry a precise d-wave symmetry can be defined with respect to the C_4 rotational symmetry about the axis of the cylinder. Indeed, looking at the long-distance behavior of the pair-field correlation function, we distinguish two cases, as shown schematically in Fig. 8: correlations can be said to be "d-wave" if they are odd under this C_4 rotation, and "d-wave-like" if they are even under rotation, but have opposite signs on the x and y directed bonds. The long-distance behavior of the correlation function corresponds to true d-wave symmetry everywhere in the phase diagram except in the CDW-4d, liquid I, and liquid II. Of these, the first two show clear d-wave-like symmetry, while liquid II cannot be easily classified by symmetry at all. Note that these are the phases which have weak or vanishing charge order.

The $\Phi_{y,y}$ ($\Phi_{y,x}$) correlation function is shown in Fig. 9 along the y (x) bonds for (a) the CDW-4a phase ($t_2 = J_2 = 0$) and (b) the CDW-4d phase ($t_2 = 1/6$ and $J_2 = 0$) of the t-J model with respect to the vertical black bond at the bottom left corner. The long-distance sign pattern of the superconducting correlations demonstrates d-wave and d-wave-like symmetries matching Fig. 8. We have confirmed this pattern by applying an external pair field $D_{\vec{a}}(\vec{r}_i)$ along one rung at the edge of the cylinder and measuring the response in the system bulk (see Supplemental Material Fig. S9).

C. Pair-field oscillation

The superconducting pair-field correlations show varying degrees of oscillation across the phase diagrams with and without flux. The pair-field component $\phi_{\vec{Q}}$ at nonzero wave vector $\vec{Q}$ can couple to the CDW order parameter $\rho_{\vec{Q}}$ through terms in the energy of the form [1,57]

$$\rho_{\vec{Q}}\phi_0^*\phi_{-\vec{Q}} + \text{c.c.}, \quad \rho_{2\vec{Q}}\phi_{-\vec{Q}}^*\phi_{-\vec{Q}} + \text{c.c.}, \tag{14}$$
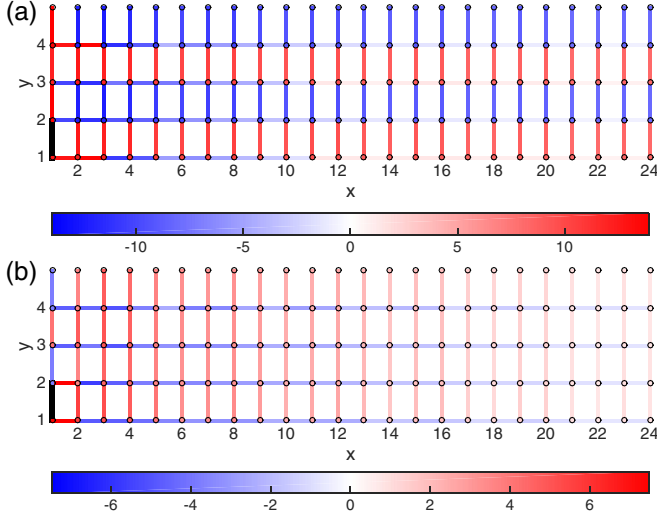
FIG. 9. Superconducting correlation functions on $L_x = 48$ cylinder for (a) CDW-4a phase with $t_2 = J_2 = 0$ and (b) CDW-4d phase with $t_2 = 1/6$ and $J_2 = 0$. The black line denotes the reference y bond and vertical (horizontal) colored lines denote $\log[1 + |\Phi_{y,y}|/|\Phi_0|]$ ($\log[1 + |\Phi_{y,x}|/|\Phi_0|]$), where Φ_0 is the minimum of the correlation function. Red (blue) is used where the correlation function is positive (negative). The change in color around the cylinder shows the sign change of the long-distance superconducting correlations which suggests d-wave symmetry in the CDW-4a phase and d-wave-like symmetry in the CDW-4d phase.

such that when two of the factors in the first term are present, the third one is also expected to be present on general grounds of Landau theory. Since the second term is quadratic in $\phi_{\bar{Q}}$, a pair-density wave (PDW) component will be accompanied by charge ordering with twice the wave vector, but the converse is not true. This indicates that the PDW is a bonafide phase which can exist independently of other orders. Observation of a superconducting component with half the CDW wave vector would have suggested an intrinsic tendency towards PDW order. However, we only find a density wave component in the correlation function $\Phi^{(dw)}$ with the same period as the CDW.

The pair-field correlations are enhanced when flux is threaded through the cylinder and exhibit oscillations in the amplitude of the superconducting correlation functions, for instance, for $J_2 = 0$ and $t_2 = 1/12$ as well as $J_2/J_1 = 0.56$ and 0.80. The period is again the same as the charge order suggesting a strong coupling between CDW and uniform SC fluctuations with correlations that can be fit to Eq. (9). We find values of $\Phi_{y,y}^{(dw)}/\Phi_{y,y}^{(sc)} \sim 0.11$–0.97 with the largest values occurring for larger J_2/J_1, e.g., $J_2/J_1 = 0.56$ and 0.80 [see Fig. 10(b) and Fig. S5 in Supplemental Material] corresponding to (weak) period 8 charge order and short-ranged $[0,\pi]$ spin order, while the pair-field oscillations are smaller for other parameters [see Fig. 10(a)]. While we do not find a finite PDW component at $Q_{cdw}/2$, the observation of an induced density wave $\Phi^{(dw)}$ comparable to the uniform superconducting component $\Phi^{(sc)}$ allows us to conclude that the coupling of the first term in Eq. (14) is significant in our model. We find $\Phi^{(dw)}/\Phi^{(sc)}$ tends to increase with larger t_2
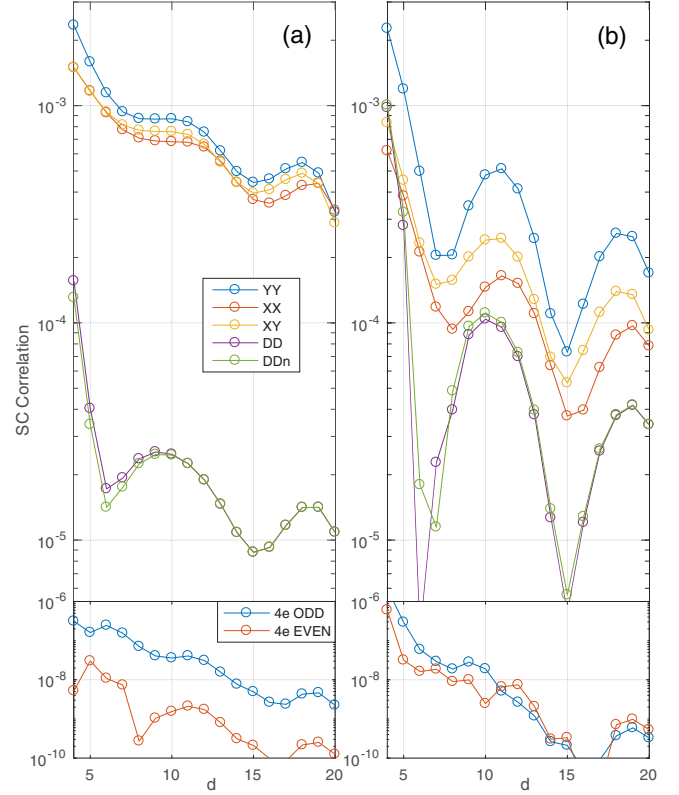

FIG. 10. Superconducting correlations for the t-J model with flux on $L_x = 48$ cylinder as a function of separation d along $\hat{x}$ for (a) $J_2 = 0.3J_1$ and $t_2 = 1/6$ showing strong uniform component $\Phi_{y,y}^{(sc)}$ and (b) $J_2 = 0.56J_1$ and $t_2 = 1/6$ showing a significant induced density wave component $\Phi_{y,y}^{(dw)}$.

when flux is threading the cylinder, which is an expected consequence of Eq. (14).

D. Charge 4e

We have also checked the correlations of the two singlet "quartet" charge 4e operators $\phi_{4e,\pm}$ as defined in Eqs. (10) and (11). The correlation function is found to decay rapidly and fall to below numerical error within a couple lattice constants across the entire phase diagram with and without flux (as can be seen, for example, in Fig. 10). Charge 4e superconductivity seems unlikely in the present model.

VII. ENERGY GAPS

Energy gaps can be determined by adding particles to the system and comparing the ground state energies. We define the energy gap Δ_m as the energy (per particle):

$$\Delta_m = \frac{1}{m}[E_0(N + m) + E_0(N - m) - 2E_0(N)], \quad (15)$$

where $E_0(N)$ is the ground state energy of the system with N particles. For a charge 2e superconductor, there is a gap to add one particle, but no gap to add two or four particles, i.e., $\Delta_1 \neq 0$ and $\Delta_2 = \Delta_4 = 0$. We compute these gaps for $L_x \times 4$ cylinders with $L_x = 8, 16, 24$ and extrapolate to $L_x \to \infty$ with a second-order polynomial fit [58]. The gaps Δ_2 and Δ_4
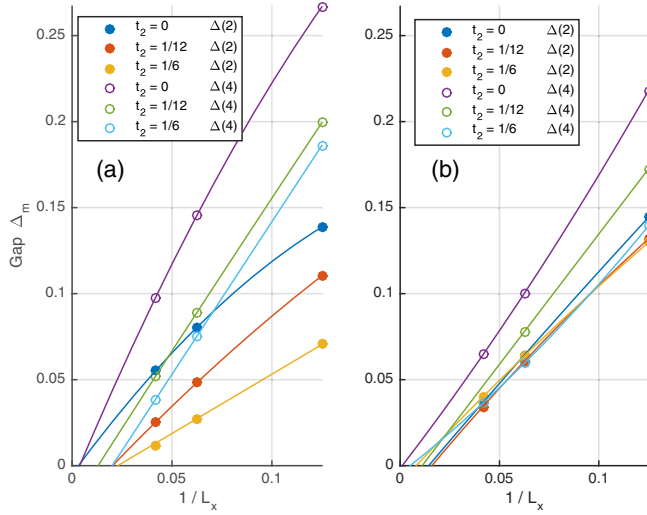
FIG. 11. Energy gap Δ_m defined in Eq. (15) of the t-J model under (a) periodic and (b) antiperiodic boundary conditions at $J_2 = 0$ and $t_2 = 0, 1/12, 1/6$.

computed from the DMRG simulations are plotted in Fig. 11 for $J_2 = 0$ and $t_2 = \{0, 1/12, 1/6\}$ (a) without and (b) with flux. The single particle gap Δ_1 for $J_2 = 0$ (not shown) is largest for $t_2 = 0$ while close to zero for $t_2 = 1/6$, where the CDW order is weaker for larger t_2. The opposite is true for the case with flux: the CDW order and single particle gap Δ_1 are largest for $t_2 \sim 1/6$. Therefore, our results suggest the presence of Cooper pairing corresponding to the finite energy gap Δ_1.

However, we find Δ_2 and Δ_4 appear to vanish upon extrapolation. This seemingly is at odds with the observed finite superconducting correlation lengths $\xi_{sc} \lesssim 10$.

VIII. DISCUSSION

A. Intertwined orders

Despite the simplicity of the model we have studied, we have unveiled a remarkably complex intertwining between at least nine forms of order (CDW-4, CDW-8, SDW-8, SDW-16, SDW $0 - \pi$, SDW $\pi - 0$, SDW $\pi - \pi$, d-wave, and d-wave-like SC). There is a general tendency for terms which depress CDW order to enhance the SC correlations, showing that there is some form of "competition" between these two orders. Where the superconducting correlations show oscillatory spatial structures, the period is always the same as that of the CDW, and hence can also be understood in terms of a competition between CDW and uniform SC orders. CDW induced oscillations of the SC order parameter similar to what we have observed have recently been imaged on the surface of Bi2212 directly by Josephson tunneling microscopy [59], and were inferred previously from features of the quasiparticle spectrum in scanning tunneling microscopy [60].

The relation between SDW and CDW order, by contrast, is less obvious. For small t_2 and no flux, we see robust period 4 CDW order. For small J_2/J_1, there are corresponding period 8 SDW correlations, but upon increasing J_2/J_1 to $\sim 1/2$, the magnetic correlations essentially disappear. The interplay be-

tween spin and charge order can produce diverse macroscopic realizations [61]. This observation offers a possible connection between the intertwined order in LSCO, lack of substantial static spin correlations in BSCCO, and apparently unrelated charge and spin ordering in YBCO. The relative insensitivity of the charge ordering to the degree of spin ordering apparent in our study supports the perspective that the charge density waves which have been observed across different families of underdoped cuprates have a common origin.

B. Origin of the density wave orders

We have studied the role of Fermi surface nesting in density wave formation on the four-leg cylinder. Since nesting is perfect in 1D and problematic in higher dimensions, the cylinder geometry we have studied represents the strongest candidate for observing nesting-induced CDW. The fact that we do not find a clear relationship between Q_{cdw} and the values of $2k_F$ suggests Fermi surface nesting does not generally play a role in CDW formation.

From the strong coupling perspective, we can view the CDW-4a (half-filled stripe) ground state as a Wigner crystal of singlet pairs which delocalize around the cylinder. The finite spin correlation length, ξ_{sdw}, can perhaps be thought of as the size of a Cooper pair, and the energy to break a pair can be associated with the single particle gap Δ_1 to add a hole to the system.

C. Doped spin liquid

Given that the spin-1/2 antiferromagnetic square $J_1 - J_2$ Heisenberg model exhibits [48–50] an intermediate quantum paramagnetic phase, and possibly contains a spin liquid subregime, we had initially hoped to see an interesting remnant of this when we doped the system, forming a "doped spin liquid." Arguments were presented by Anderson [62], and one of us [56,63] that a spin liquid can be viewed as a paired state with zero superfluid stiffness, so that upon doping it would inevitably form a strongly superconducting state. More recently, it has been proposed that a doped spin liquid might form an FL* phase, which in turn has been proposed as a candidate explanation of the physics of the pseudogap regime of the hole-doped cuprates [53,54,64]. Unfortunately, CDW order seems to be the dominant ordering tendency, even in the doped spin liquid range of parameters, and no evidence of either of these conjectured behaviors has yet been seen in our studies.

D. Superconducting symmetry

It is an interesting feature of the cylinder geometry that a true symmetry distinction between d-wave and s-wave superconducting states is possible. The superconducting correlations in our model were shown to have d-wave symmetry across the phase diagram where charge order is present, and d-wave-like symmetry—although this is technically s-wave symmetry with respect to rotation about the axis of the cylinder—where charge order is absent or weak (preliminary results on wider $L_y = 8$ cylinders for $t_2 = J_2 = 0$ show the d-wave-like symmetry pattern suggesting the d-wave pattern observed for $L_y = 4$ is unique to the cylinder geometry).

For moderate J, particles on a single plaquette tend to pair; we can therefore imagine a stack of plaquettes, each favoring one or two pairs where the two-electron ground state has s-wave symmetry and the four-electron ground state has d-wave symmetry [65]. Turning on a coupling between plaquettes, pair hopping then corresponds to a bosonic operator with d-wave symmetry which manifests in a sign change of the superconducting correlation function upon rotating the cylinder by $\pi/2$.

Away from $\delta = 1/8$, and especially for $\delta \sim 0.15$, where the CDW ordering tendencies are weaker, in agreement with other studies of t-J ladders [36], we observe substantially enhanced SC correlations, as we will report in a separate paper.

[1] See, for example, E. Fradkin, S. A. Kivelson, and J. M. Tranquada, Rev. Mod. Phys. **87**, 457 (2015).

[2] S. R. White, Phys. Rev. Lett. **69**, 2863 (1992).

[3] S. R. White, Phys. Rev. B **48**, 10345 (1993).

[4] S. R. White, I. Affleck, and D. J. Scalapino, Phys. Rev. B **65**, 165122 (2002).

[5] For a recent summary, see B. Keimer, S. A. Kivelson, M. R. Norman, S. Uchida, and J. Zaanen, Nature (London) **518**, 179 (2015).

[6] J. M. Tranquada, B. J. Sternlieb, J. D. Axe, Y. Nakamura, and S. Uchida, Nature (London) **375**, 561 (1995).

[7] R. J. Birgeneau, C. Stock, J. M. Tranquada, and K. Yamada, J. Phys. Soc. Jpn. **75**, 111003 (2006).

[8] J. M. Tranquada, Physica B **407**, 1771 (2012).

[9] S. Blanco-Canosa, A. Frano, T. Loew, Y. Lu, J. Porras, G. Ghiringhelli, M. Minola, C. Mazzoli, L. Braicovich, E. Schierle, E. Weschke, M. Le Tacon, and B. Keimer, Phys. Rev. Lett. **110**, 187001 (2013).

[10] M. Hücker, N. B. Christensen, A. T. Holmes, E. Blackburn, E. M. Forgan, R. Liang, D. A. Bonn, W. N. Hardy, O. Gutowski, M. v. Zimmermann, S. M. Hayden, and J. Chang, Phys. Rev. B **90**, 054514 (2014).

[11] S. Blanco-Canosa, A. Frano, E. Schierle, J. Porras, T. Loew, M. Minola, M. Bluschke, E. Weschke, B. Keimer, and M. Le Tacon, Phys. Rev. B **90**, 054513 (2014).

[12] Y. Y. Peng, M. Salluzzo, X. Sun, A. Ponti, D. Betto, A. M. Ferretti, F. Fumagalli, K. Kummer, M. Le Tacon, X. J. Zhou, N. B. Brookes, L. Braicovich, and G. Ghiringhelli, Phys. Rev. B **94**, 184511 (2016).

[13] V. Thampy, S. Blanco-Canosa, M. Garcia-Fernandez, M. P. M. Dean, G. D. Gu, M. Forst, T. Loew, B. Keimer, M. Le Tacon, S. B. Wilkins, and J. P. Hill, Phys. Rev. B **88**, 024505 (2013).

[14] J. Zaanen and O. Gunnarsson, Phys. Rev. B **40**, 7391 (1989).

[15] H. J. Schulz, Phys. Rev. Lett. **64**, 1445 (1990).

[16] K. Machida, Physica C **158**, 192 (1989).

[17] V. J. Emery and S. A. Kivelson, Physica C **209**, 597 (1993).

[18] U. Löw, V. J. Emery, K. Fabricius, and S. A. Kivelson, Phys. Rev. Lett. **72**, 1918 (1994).

[19] J. Zaanen, J. Phys. Chem. Solids **59**, 1769 (1998).

[20] S. R. White and D. J. Scalapino, Phys. Rev. Lett. **80**, 1272 (1998).

[21] S. R. White and D. J. Scalapino, Phys. Rev. B **60**, R753(R) (1999).

[22] M. Troyer, H. Tsunetsugu, and T. M. Rice, Phys. Rev. B **53**, 251 (1996).

[23] O. Zachar, S. A. Kivelson, and V. J. Emery, Phys. Rev. B **57**, 1422 (1998).

[24] D. J. Scalapino and S. R. White, Physica C **481**, 146 (2012).

[25] P. Schmitteckert and R. Werner, Phys. Rev. B **69**, 195115 (2004).

[26] M. D. Johannes and I. I. Mazin, Phys. Rev. B **77**, 165135 (2008).

[27] R. Comin, A. Frano, M. M. Yee, Y. Yoshida, H. Eisaki, E. Schierle, E. Weschke, R. Sutarto, F. He, A. Soumyanarayanan, Y. He, M. Le Tacon, I. S. Elfimov, J. E. Hoffman, G. A. Sawatzky, B. Keimer, and A. Damascelli, Science **343**, 390 (2014).

[28] Y. Wang and A. Chubukov, Phys. Rev. B **90**, 035149 (2014).

[29] C. Pepin, V. S. de Carvalho, T. Kloss, and X. Montiel, Phys. Rev. B **90**, 195207 (2014).

[30] S. Whitsitt and S. Sachdev, Phys. Rev. B **90**, 104505 (2014).

[31] O. F. Syljuasen, S. Chakravarty, and M. Greven, Phys. Rev. Lett. **78**, 4115 (1997).

[32] S. Chakravarty, Phys. Rev. Lett. **77**, 4446 (1996).

[33] G. Ghiringhelli, M. Le Tacon, M. Minola, S. Blanco-Canosa, C. Mazzoli, N. B. Brookes, G. M. De Luca, A. Frano, D. G. Hawthorn, F. He, T. Loew, M. Moretti Sala, D. C. Peets, M. Salluzzo, E. Schierle, R. Sutarto, G. A. Sawatzky, E. Weschke, B. Keimer, and L. Braicovich, Science **337**, 821 (2012).

[34] J. Chang, E. Blackburn, A. T. Holmes, N. B. Christensen, J. Larsen, J. Mesot, R. Liang, D. A. Bonn, W. N. Hardy, A. Watenphul, M. v. Zimmermann, E. M. Forgan, and S. M. Hayden, Nat. Phys. **8**, 871 (2012).

[35] E. H. da Silva Neto, P. Aynajian, A. Frano, R. Comin, E. Schierle, E. Weschke, A. Gyenis, J. Wen, J. Schneeloch, Z. Xu, S. Ono, G. Gu, M. Le Tacon, and A. Yazdani, Science **343**, 393 (2014).

[36] S. R. White and D. J. Scalapino, Phys. Rev. B **55**, R14701(R) (1997).

[37] Short period PDW correlations with power-law fall-off were found previously in DMRG studies of asymmetric two leg ladders [38,39].

[38] E. Berg, E. Fradkin, and S. A. Kivelson, Phys. Rev. Lett. **105**, 146403 (2010).

[39] A. Jaefari and E. Fradkin, Phys. Rev. B **85**, 035104 (2012).

[40] M. S. Chang and I. Affleck, Phys. Rev. B **76**, 054521 (2007).

[41] C. M. Varma, Phys. Rev. B **55**, 14554 (1997).

[42] S. Chakravarty, R. B. Laughlin, D. K. Morr, and C. Nayak, Phys. Rev. B **63**, 094503 (2001).

[43] See Supplemental Material at http://link.aps.org/supplemental/10.1103/PhysRevB.95.155116 for Fig. S3 for example.

[44] See Supplemental Material at http://link.aps.org/supplemental/10.1103/PhysRevB.95.155116 for Figs. S1 and S2 for details.

[45] An alternative definition for the correlation length which we have studied is $\xi_{sdw}(\vec{Q},\vec{q}_{min}) = \frac{1}{|\vec{q}_{min}|}\sqrt{\frac{S(\vec{Q})}{S(\vec{Q}+\vec{q}_{min})} - 1}$, where $\vec{Q}$ is the peak and $|\vec{q}_{min}| = 2\pi/L_x$. While there are small quantitative differences that result from the use of this alternative definition, it does not make a qualitative difference.

[46] See Supplemental Material at http://link.aps.org/supplemental/10.1103/PhysRevB.95.155116 for Fig. S4 for details.

[47] F. Figueirido, A. Karlhede, S. Kivelson, S. Sondhi, M. Rocek, and D. S. Rokhsar, Phys. Rev. B **41**, 4619 (1990).

[48] H. C. Jiang, H. Yao, and L. Balents, Phys. Rev. B **86**, 024424 (2012).

[49] S. S. Gong, W. Zhu, D. N. Sheng, O. I. Motrunich, and M. P. A. Fisher, Phys. Rev. Lett. **113**, 027201 (2014).

[50] L. Wang, Z. C. Gu, F. Verstraete, and X. G. Wen, Phys. Rev. B **94**, 075143 (2016).

[51] M. Yamanaka, M. Oshikawa, and I. Affleck, Phys. Rev. Lett. **79**, 1110 (1997).

[52] E. Lieb, T. Schultz, and D. Mattis, Ann. Phys. (N.Y.) **16**, 407 (1961).

[53] T. Senthil, S. Sachdev, and M. Vojta, Phys. Rev. Lett. **90**, 216403 (2003).

[54] M. Punk, A. Allais, and S. Sachdev, Proc. Natl. Acad. Sci. USA **112**, 9552 (2015).

[55] J. Lee, S. Sachdev, and S. R. White, Phys. Rev. B **94**, 115112 (2016).

[56] D. S. Rokhsar and S. A. Kivelson, Phys. Rev. Lett. **61**, 2376 (1988).

[57] E. Berg, E. Fradkin, and S. A. Kivelson, Phys. Rev. B **79**, 064515 (2009).

[58] E. M. Stoudenmire and S. R. White, Annu. Rev. Condens. Matter Phys. **3**, 111 (2012)

[59] M. H. Hamidian, S. D. Edkins, S. H. Joo, A. Kostin, H. Eisaki, S. Uchida, M. J. Lawler, E. A. Kim, A. P. Mackenzie, K. Fujita, J. Lee, and J. C. Seamus Davis, Nature (London) **532**, 343 (2016).

[60] C. Howald, H. Eisaki, N. Kaneko, M. Greven, and A. Kapitulnik, Phys. Rev. B **67**, 014533 (2003).

[61] J. Zaanen, O. Y. Osman, H. V. Kruis, Z. Nussinov, and J. Tworzydlo, Philos. Mag. B **81**, 1485 (2001).

[62] P. W. Anderson, Science **235**, 1196 (1987).

[63] S. A. Kivelson, D. S. Rokhsar, and J. P. Sethna, Phys. Rev. B **35**, 8865(R) (1987).

[64] D. Chowdhury and S. Sachdev, arXiv:1605.03579.

[65] D. J. Scalapino and S. A. Trugman, Philos. Mag. B **74**, 607 (1996).